

# Portlandite solubility and $\text{Ca}^{2+}$ activity in presence of gluconate and hexitols

BOUZOUAID Lina<sup>1</sup>, LOTHENBACH Barbara<sup>2</sup>, FERNANDEZ-MARTINEZ Alejandro<sup>3</sup>, LABBEZ Christophe<sup>1</sup>

<sup>1</sup> ICB, UMR 6303 CNRS, Univ. Bourgogne Franche-Comté, FR-21000 Dijon, France

<sup>2</sup> Empa, Concrete & Asphalt Laboratory, Dubendorf, Switzerland

<sup>3</sup> Univ. Grenoble Alpes, Univ. Savoie Mont Blanc, CNRS, IRD, IFSTTAR, ISTerre, 38000 Grenoble, France.

## Abstract

The current paper investigates the impact of gluconate, D-sorbitol, D-mannitol and D-galactitol on calcium speciation at high pH values by i) solubility measurements of portlandite ( $\text{Ca}(\text{OH})_2$ ) and ii) potentiometric titration measurements of calcium salt solutions. Thermodynamic modeling was used to fit the chemical activities of  $\text{Ca}^{2+}$  and  $\text{OH}^-$  ions and thus to determine the strength and kind of the different Ca-organic-hydroxide complexes. The strength of complex formation with Ca decreases in the order gluconate  $\gg$  sorbitol  $>$  mannitol  $>$  galactitol, which follows the same order as sorption on portlandite. Heteropolynuclear gluconate complexes with calcium and hydroxide dominate the Ca-speciation in the presence of portlandite, while for sorbitol ternary  $\text{CaSorbOH}^+$  complexes were dominant under alkaline conditions. We expect that these results will help in better understanding the influence of gluconate and hexitols on the hydration of alite and Portland cement.

## 21 **1. Introduction**

22 The chemical activity of ions,  $a$ , and the solubility of minerals are crucial factors in determining the  
23 thermodynamic conditions and the driving force of a mineral to dissolve or to precipitate (1). The  
24 extent to which a solution is out of equilibrium is given by the deviation from the theoretical  
25 solubility and is quantified by the saturation index. For a solid such as portlandite, of solubility  
26 product  $K_{Ca(OH)_2}$ , the saturation index (SI) is defined as:

27

$$SI = \log(a_{Ca^{2+}} \cdot a_{OH^-}^2 / K_{Ca(OH)_2})$$

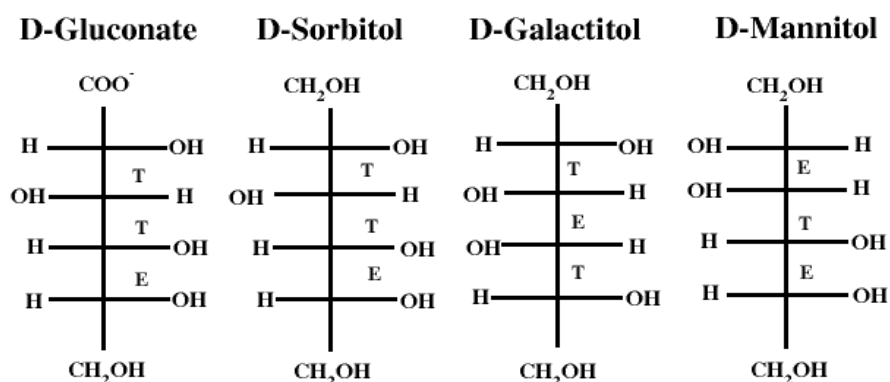
28 The knowledge of the elemental concentrations, the speciation and the ion activities provides a  
29 simple measure for the driving force of dissolution or precipitation reactions. However, activity of  
30 ions is sensitive to the presence of other chemical species via the effect of ionic strength. Many ions  
31 can also form different soluble complexes such as e.g. calcium gluconate complexes:  $Ca\text{gluc}^+$ ,  
32  $Ca(\text{gluc})_2^0$ , ... and can in addition promote or inhibit crystal growth/dissolution, which can make the  
33 determination of the activity of ions difficult and tedious.

34 In the case of concrete, organic molecule inhibitors, called retarders, are commonly used in specific  
35 applications (2) (3) (4) to delay the cement setting. Superplasticizers, often comb co-polymers,  
36 employed in the formulation of ultra high performance concrete, are also known to retard the curing  
37 of concrete (5) (6) (7). Although used in low amount, less than 1 wt.% of Portland cement (8), the  
38 concentration of organic molecules in the solution present in the interstitial pores formed by cement  
39 grains, easily reaches several tens of millimolar concentrations during the first hours after mixing  
40 with water and can thus impact the cement reactions involved in the curing. These effects have been  
41 illustrated in several studies with various organic molecules (9) (10). Invariably, it was found that  
42 the organic molecules acting as cement curing inhibitors can greatly influence the elemental  
43 concentrations in the aqueous pore solution and retard the cement hydration. The cement hydration  
44 is complex and dependent on two interrelated and concomitant processes, which are the dissolution  
45 of the cement grains and the precipitation of the hydrates. However, the physical and chemical  
46 mechanisms responsible for this retardation are not fully understood (11) (12) (13) (14) (15).

47 Furthermore, in those organic-cement systems, an accurate quantification of the dissolution rate of  
 48 cement anhydrides and precipitation rate of cement hydrates at well-defined *SI* is still missing as a  
 49 result of limited knowledge of complex formation.

50 For the organics of interest in this paper, the pure dissolution of alite ( $\text{Ca}_3\text{SiO}_5$ ) was found to be  
 51 negligibly affected by gluconate and three different hexitols, namely sorbitol, mannitol and  
 52 galactitol (15). These organics, however, have a great impact on alite hydration and to a less extend  
 53 on the hydration of Portland cement (15). These molecules were thus conjectured to mostly act as  
 54 nucleation-growth inhibitors of calcium silicate hydrate, C-S-H (16) In a recent experimental study,  
 55 it was suggested that the inhibition of the crystallization of portlandite,  $\text{Ca}(\text{OH})_2$ , could be the main  
 56 reason of the slowdown of alite hydration (17).

57



58

59 Figure 1: Structure of (from left to right) D-gluconate, D-sorbitol, D-galactitol and D-mannitol. "T"  
 60 corresponds to the threo diastereoisomer configuration. "E" corresponds to erythro diastereoisomer  
 61 configuration.

62

63 Gluconate, a negatively charged molecule, was found to be a stronger retardant of cement hydration  
 64 than neutral hexitols (16) (18) (19). For different hexitols also the stereochemical arrangements of  
 65 the organic molecules, as illustrated in Figure 1, has an influence (16). The retardation was  
 66 observed to increase from mannitol to galactitol to sorbitol, which have the same chemical  
 67 composition and functional groups, but a different arrangement. However, the chemical  
 68 mechanisms, which could explain how these organics retard are poorly understood, e.g. their impact  
 69 on the anhydrate and hydrate solubility and the eventual formation of aqueous complexes [ (16)

70 (18)]. In particular, in the high pH range little is known about possible aqueous complexes with  
71 organic molecules or their stability.  
72 It has been suggested that the ability of the organic molecules to form complexes with  $\text{Ca}^{2+}$  is  
73 directly correlated to their adsorption affinity with calcium rich surfaces of C-S-H and alite (18)  
74 (19) which, in turn, may impart the surface tension of the nucleus or the rate of attachment of  
75 species to the nucleus and, thus, the nucleation rate. Thus, the understanding and quantification of  
76 complex formation between organic molecules and calcium could be fundamental for a better  
77 understanding of the observed retardation by organic additives<sup>1</sup>. In addition, only an adequate  
78 quantification of the different Ca-complexes formed in the presence of organics makes it possible to  
79 determine the ion activities needed to calculate *SI* with respect to  $\text{Ca}_3\text{SiO}_5$ , calcium silicate hydrate  
80 and portlandite.

81 D-gluconate, is a well know retarding additive (20) (21) (22) widely used in the industry. In  
82 addition to its role as retarder in cements and concretes, gluconate is also used for water treatment  
83 and metal surface treatment due its strong complexation ability with cations. The complex  
84 formation between Ca and gluconate has been investigated in several studies (23) (24) (25) (26)  
85 (27) (28), but mainly at high ionic strength (1.0 M NaCl) and relatively low pH. On the other hand,  
86 the complex formation between hexitols and calcium ions was much less investigated (29) (30) and  
87 again at relatively low pH values not relevant for cements.

88 The present paper thus aims to investigate the speciation of alkaline calcium solutions in the  
89 presence of a carboxylate sugar acid: gluconate and several uncharged hexitols: D-sorbitol (D-  
90 glucitol), D-mannitol, and D-galactitol, at concentrations and pH values relevant for cementitious  
91 systems. A particular emphasis is on the ability of the organics to form complexes with calcium  
92 ions. This is assessed experimentally by solubility measurements of portlandite and ion activity  
93 measurements of alkaline calcium solutions in presence of increasing amount of organics. The  
94 results were then fitted with a speciation model, using the open source software PHREEQC, to  
95 determine the strength and the various types of calcium complexes with the organic molecules.

---

1 <sup>1</sup> Numerous more effects may impart a retardation of cement hydration

96

## 97 **2. Materials and methods**

### 98 *2.1 Materials*

99 The different stock solutions from each compound were prepared by dissolving  $\text{Ca}(\text{NO}_3)_2 \cdot 4\text{H}_2\text{O}$   
100 (Sigma-Aldrich,  $\geq 99\%$  purity), potassium gluconate ( $\text{C}_6\text{H}_{11}\text{KO}_7$ , Sigma-Aldrich,  $\geq 99\%$  purity) D-  
101 sorbitol ( $\text{C}_6\text{H}_{14}\text{O}_6$ , Sigma-Aldrich,  $\geq 99\%$  purity), D-mannitol ( $\text{C}_6\text{H}_{14}\text{O}_6$ , Sigma-Aldrich,  $\geq 99\%$   
102 purity), and D-galactitol ( $\text{C}_6\text{H}_{14}\text{O}_6$ , Sigma-Aldrich,  $\geq 99\%$  purity), in boiled and degassed milliQ  
103 water. In the potentiometric titration experiments, potassium nitrate ( $\text{KNO}_3$ , Sigma-Aldrich,  $\geq 99\%$   
104 purity) was used as a background electrolyte (0.1 M) and KOH ( $>85\%$ , Sigma-Aldrich) to increase  
105 the pH values to 11.3, 12.3, 12.7 and 13.0. For the solubility measurement, portlandite, calcium  
106 hydroxide ( $\text{Ca}(\text{OH})_2$ , Sigma-Aldrich,  $\geq 95\%$ ) was used.

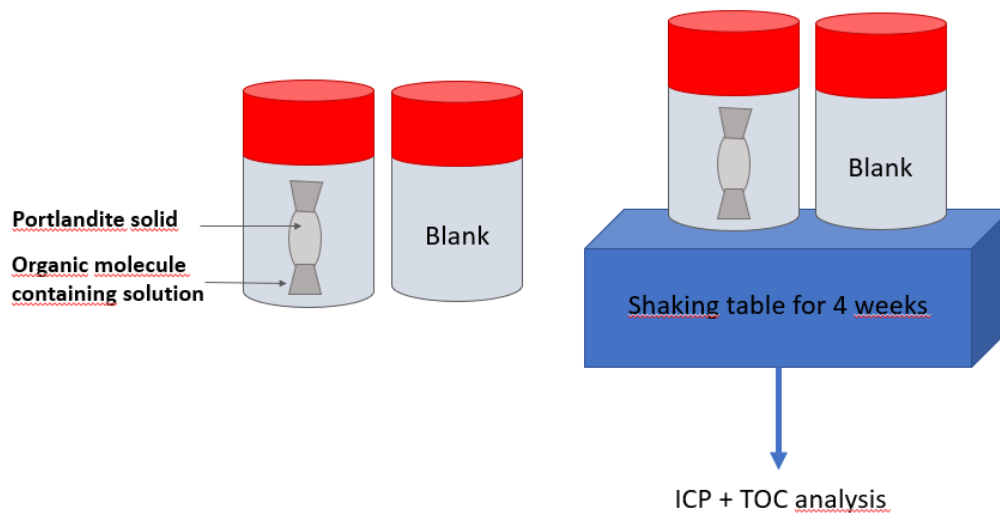
107 It is important to note that the hexitols used in this study are all isomers, sharing the formula,  
108  $\text{HOCH}_2(\text{CHOH})_4\text{CH}_2\text{OH}$ , but differ in the stereochemical arrangement of the OH groups as  
109 illustrated in Figure 1.

110

### 111 *2.2 Solubility experiments*

112 For the solubility experiments, various series of samples were prepared in a glove box with 3.92 g  
113 of  $\text{Ca}(\text{OH})_2$ , as a solid buffer, enclosed in a dialysis membrane and then placed in a 250 mL  
114 polypropylene flask filled with 200 mL of  $\text{CO}_2$ -free solution with different amounts and type of  
115 organic molecule, see Figure 2. Prior to use, the dialysis membranes (Spectra / Por, MWCO 12-14  
116 kD) were dipped in distilled water for 30 minutes to remove any organic residues and dried in a  
117 desiccator overnight; the dialysis bags were closed with polyamide clamps (Carl Roth, length 50  
118 mm). Finally, the samples were stored in a 16 L plastic barrel filled with  $\text{N}_2$  gas, to guarantee  $\text{CO}_2$   
119 free conditions, and placed on a shaking table during four weeks at  $23^\circ\text{C}$  to ensure a proper  
120 equilibrium.

121



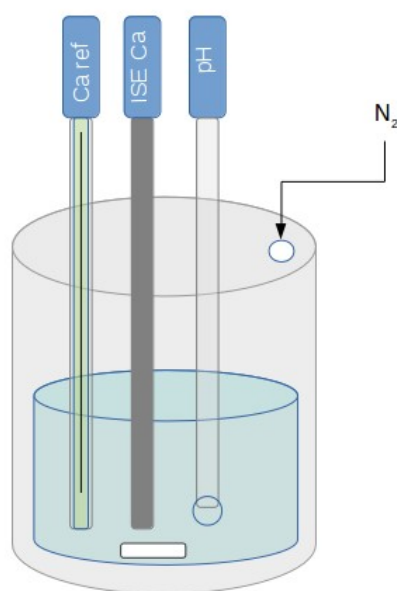
123 Figure 2: Schematic representation of a pair of samples used for the solubility and adsorption  
 124 experiments. The flask used for the solubility measurement contains a dialysis bag filled with  
 125 portlandite powder, immersed in a solution containing the organic molecule. The second flask  
 126 contains the organic molecule solution only and is used as a blank/reference to verify the organic  
 127 concentration introduced initially. This allows the determination of the organic adsorption on C-S-H  
 128 by mass balance based on the measured difference. Note that the same stock solution is used for  
 129 each sample pair.  
 130

131 The pH values were recorded after removing the dialysis bags from the bottles. The pH electrode  
 132 (Consort C931 electrochemical analyser) was calibrated using Sigma Aldrich buffer ( pH 4, 7, 9 and  
 133 12). The total concentration of the elements Ca and Si was measured by inductively coupled  
 134 plasma-optic emission spectroscopy (ICP-OES 5110, Agilent). The bulk concentration of organics  
 135 at equilibrium was measured as total organic content with a TOC VCPN instrument (Shimadzu).  
 136 This method is based on the oxidation of organic molecules contained in solution by gaseous  
 137 oxygen with a platinum-based catalyst in an oven raised to a temperature of 720°C. The CO<sub>2</sub>  
 138 formed is detected by Infra-Red Non-Dispersive (NDIR). The detection threshold for this device is  
 139 very low (4µg/L).  
 140

### 141 2.3 Titration of Ca<sup>2+</sup> with the ion selective electrode

142 The chemical activity of calcium ions was also determined from potentiometric titration  
 143 measurements using an automatic titrator instrument (Metrohm 905 Titrando); the setup is detailed  
 144 in Figure 3. All measurements were performed in a titration reactor thermostated to 23.0 ± 0.1°C.

145 The titrated solutions were continuously stirred at a constant rate 430 rpm. A nitrogen flow  
146 circulated continuously above the solution to avoid the ingress of CO<sub>2</sub>. It was taken care that the gas  
147 did not enter the solution to avoid any disturbance of the electrodes. In the reactor, 100 mL of a  
148 solution containing 0.1 M KNO<sub>3</sub> background electrolyte and 0.25 mM Ca(NO<sub>3</sub>)<sub>2</sub> was thermostated  
149 for approximately 20 minutes before the start of the titration. After 3 minutes of equilibration time,  
150 and only if the change in the electrode signal was < 0.5 mV/min, a titrant solution containing 0.2M  
151 of organic molecule was added drop by drop (0.2 ml, 50 times for a total volume added of 10 ml) at  
152 the maximal speed registered in the software "Tiamo" (Metrohm).  
153



154 Figure 3: Schematic representation of the experimental titration set up: the reactor contains the  
155 titrated solution, the calcium specific electrode, the reference electrode, and the pH electrode.  
156

157 The Ca<sup>2+</sup> activity was measured at 23.0 ± 0.1°C with a calcium sensitive electrode (Metrohm Ca  
158 ISE, 6.0508.110) coupled to a reference electrode (Metrohm Ag, AgCl/3 M KCl, 6.0750.100). A  
159 stable electrode signal could only be obtained with the use of a background electrolyte. The  
160 titrations were thus performed in 0.1 M KNO<sub>3</sub> to ensure a stable signal and to limit the influence of  
161 the background electrolyte on the complex formation. We have chosen potassium nitrate as K<sup>+</sup>  
162 interferes less with the Ca<sup>2+</sup>- selective electrode than Na<sup>+</sup> (31). The Ca<sup>2+</sup> electrode was calibrated  
163 prior to the measurements by a titration of 100 mM KNO<sub>3</sub> solution with a solution containing 500

164 mM Ca(NO<sub>3</sub>)<sub>2</sub> (0.2 ml, 50 times for a total volume added of 10 ml) and by plotting the measured  
 165 mV against the calculated Ca<sup>2+</sup> activity calculated with PHREEQC as detailed below. The response  
 166 of the Ca<sup>2+</sup> electrode was found to be linear with a slope of 29±1 mV, which corresponds to the  
 167 expected slope of 29.4 mV at 23°C. The pH was determined with a pH electrode (Metrohm pH  
 168 Unitrode with Pt 1000, 6.0259.100), which allows reliable measurements up to pH = 14. The pH  
 169 electrode was calibrated prior to the measurements with standard buffer solutions (pH 9, 10, and  
 170 12.45 from Sigma Aldrich).

171

#### 172 2.4 Thermodynamic simulation and complexation constants

173 **Table 1.** Complex formation constants K, expressed in log K, between calcium and gluconate  
 174 (Gluc<sup>-</sup>) at standard conditions (1 bar, 25°C) reported in literature and determined in the present  
 175 study.

	Sayer (28) 0M	Masone (27) (0.5M) 0M <sup>1</sup>	Zhang (35) (0.1M) 0M	Pallagi (24) (1M) 0M	Bretti (36) 0M	Kutus (26) (1M) 0M	This study 0 M
<u>Solid</u>							
Ca <sup>2+</sup> + 2OH <sup>-</sup> = Ca(OH) <sub>2</sub>	-	-	-	-	-	-	<b>-5.20<sup>a</sup></b>
<u>Aqueous complexes</u>							
Ca <sup>2+</sup> + OH <sup>-</sup> = CaOH <sup>+</sup>	-	-	-	(0.97) 1.83	-	-	<b>1.22<sup>a</sup></b>
GlucH <sup>0</sup> = Gluc <sup>-</sup> + H <sup>+</sup>	3.7	-	(3.30) 3.53	(3.24) 3.64 <sup>b</sup>	3.71	-	<b>3.64</b>
Gluc <sup>-</sup> + OH <sup>-</sup> = GlucOH <sup>2-</sup> <sup>c</sup>	-	-	-	(0.08) -0.44	-	-	<b>-0.44</b>
Ca <sup>2+</sup> + Gluc <sup>-</sup> = CaGluc <sup>+</sup>	1.21	(1.05) 1.79	-	(0.37) 1.23	-	(0.70) 1.56	<b>1.56</b>
Ca <sup>2+</sup> + 2Gluc <sup>-</sup> = CaGluc <sub>2</sub> <sup>0</sup>	-	(1.88) 2.98	-	-	-	(1.65 <sup>d</sup> ) 2.9	<b>2.85</b>
Ca <sup>2+</sup> + OH <sup>-</sup> + Gluc <sup>-</sup> = CaGlucOH <sup>0</sup>	-	-	-	(2.82) 4.07	-	(2.86 <sup>d</sup> ) 4.11	<b>3.95<sup>e</sup></b>
2Ca <sup>2+</sup> + 3 OH <sup>-</sup> + Gluc <sup>-</sup> = Ca <sub>2</sub> Gluc(OH) <sub>3</sub> <sup>0</sup>	-	-	-	(8.04) 10.48	-	-	-
2Ca <sup>2+</sup> + 4 OH <sup>-</sup> + 2Gluc <sup>-</sup> = Ca <sub>2</sub> Gluc <sub>2</sub> (OH) <sub>4</sub> <sup>2-</sup>	-	-	-	-	-	(9.49 <sup>d</sup> ) 11.34	<b>11.25<sup>e</sup></b>
3Ca <sup>2+</sup> + 4 OH <sup>-</sup> + 2Gluc <sup>-</sup> = Ca <sub>3</sub> Gluc <sub>2</sub> (OH) <sub>4</sub> <sup>0</sup>	-	-	-	(12.44) 16.07	-	(12.59 <sup>d</sup> ) 16.22	<b>16.10<sup>e</sup></b>

176 Values reported for I = 0.1, 0.5 and 1 M extrapolated to 0 M ionic strength in this study using the WATEQ Debye  
 177 Huckel equation (1); - : not reported; <sup>a</sup> values from Thoenen et al. (37); <sup>b</sup> value from Pallagi et al. (23); <sup>c</sup> notation  
 178 GlucOH<sup>2-</sup> represents the two times deprotonated C<sub>6</sub>O<sub>7</sub>H<sub>10</sub><sup>2-</sup> as suggested in (24) ; <sup>d</sup> recalculated from reaction  
 179 formulated with H<sup>+</sup> (26) using a log K<sub>w</sub> of -13.62 at 1 M NaCl; <sup>e</sup> fitted in this study



180 The solubility of portlandite and the activity of  $\text{Ca}^{2+}$  were fitted with a speciation model solved by  
 181 the geochemical software PHREEQC version 3 (3.6.2-15100) (32) and the WATEQ4f database  
 182 (33). The activity of the  $\text{Ca}^{2+}$ ,  $a_{\text{Ca}^{2+}}$ , and all other species was calculated according to  $a_{\text{Ca}^{2+}} =$   
 183  $\gamma_{\text{Ca}^{2+}} \cdot m_{\text{Ca}^{2+}}$ , where  $\gamma_{\text{Ca}^{2+}}$  is the activity coefficient and  $m_{\text{Ca}^{2+}}$  the molality in mol/kg  $\text{H}_2\text{O}$ . The  
 184 activity coefficients were calculated with the WATEQ Debye Hückel equation:

$$185 \quad \log \gamma_i = \frac{-A_y z_i^2 \sqrt{I}}{1 + B_y a_i \sqrt{I}} + b_y I \quad (1)$$

186 where  $z_i$  denotes the charge of species  $i$ ,  $I$  is the effective molal ionic strength, while  $a_i$ , the ion-size  
 187 parameter, and  $b_y$  are ion specific parameters and  $A_y$  and  $B_y$  are pressure- and temperature-  
 188 dependent coefficients (33). This activity correction is applicable up to approximately 1 M of ionic  
 189 strength (34).

190 **Table 2.** Complex formation constants, expressed in log K, between calcium and sorbitol (Sorb),  
 191 mannitol (Man) and galactitol (Gal) at standard conditions (1 bar, 25°C) reported in literature and  
 192 determined in the present study.

	Kieboom (30) (0.2-0.8M) 0M	Haas (29) (0.7M) 0M	Kutus (25) (1M) 0M	This study 0M
$\text{Ca}^{2+} + \text{Sorb}^0 = \text{CaSorb}^{2+}$	(0.11) 0.08	(-0.52) -0.54	(0) -0.06	<b>0.10<sup>a</sup></b>
$\text{Ca}^{2+} + \text{Sorb}^0 + \text{OH}^- = \text{SorbCaOH}^+$				<b>2.85<sup>a</sup></b>
$2 \text{Ca}^{2+} + 2\text{Sorb}^0 + 4\text{OH}^- =$ $\text{Ca}_2\text{Sorb}_2(\text{OH})_4^0$				<b>9.75<sup>a</sup></b>
$\text{Ca}^{2+} + \text{Man}^0 = \text{CaMan}^{2+}$	(-0.05) -0.08	(-0.62) -0.64	(-0.3) -0.36	<b>-0.36</b>
$\text{Ca}^{2+} + \text{Man}^0 + \text{OH}^- = \text{CaManOH}^+$				<b>2.65<sup>a</sup></b>
$2 \text{Ca}^{2+} + 2\text{Man}^0 + 4\text{OH}^- =$ $\text{Ca}_2\text{Man}_2(\text{OH})_4^0$				<b>9.65<sup>a</sup></b>
$\text{Ca}^{2+} + \text{Gal}^0 = \text{CaGal}^{2+}$		(-0.51) -0.53		<b>-0.53</b>
$\text{Ca}^{2+} + \text{Gal}^0 + \text{OH}^- = \text{CaGalOH}^+$				<b>2.80<sup>a</sup></b>
$2 \text{Ca}^{2+} + 2\text{Gal}^0 + 4\text{OH}^- = \text{Ca}_2\text{Gal}_2(\text{OH})_4^0$				<b>9.29<sup>a</sup></b>

193 <sup>a</sup>Fitted in this study

194 The complex formation constants between  $\text{Ca}^{2+}$  and hydroxide, gluconate, sorbitol, mannitol and  
 195 galactitol reported in the literature and determined in the present study are detailed in Table 1 and  
 196 Table 2. For gluconate, sorbitol and mannitol we used as starting values the complexes and  
 197 associated constants derived from Pallagi and co-workers (23) (24) (25) (26). They were, where

198 necessary, further refined to obtain a good visual fit between the measured and the modeled data.  
199 The following procedure to refine the complexation constants was employed. First, the  
200 potentiometric data measured at pH 11.3 were used to fit the constants for the  $\text{CaGluc}^+$ ,  $\text{CaSorb}^{2+}$ ,  
201  $\text{CaMan}^{2+}$ , and  $\text{CaGal}^{2+}$  complexes, which dominate at low pH values. Then, the titration data at  
202 higher pH values were used to fit the constants for the  $\text{CaGlucOH}^0$ ,  $\text{CaSorbOH}^+$ ,  $\text{CaManOH}^+$ , and  
203  $\text{CaGalOH}^+$  complexes. The formation of  $\text{CaGluc}_2^0$ , suggested by Pallagi et al. (23) and Kutus et al.  
204 (26), and of  $\text{Ca}_2\text{Gluc}_2\text{OH}_4^{2-}$  and  $\text{Ca}_3\text{Gluc}_2\text{OH}_4^0$  complexes suggested by Kutus et al. (26), were also  
205 considered. Only traces of the  $\text{CaGluc}_2^0$  complex were calculated to be present in our experiments  
206 (less than 1 % of the total Ca in any of the experiments) thus this complex was considered but its  
207 constant not further refined. The presence of  $\text{Ca}_3\text{Gluc}_2\text{OH}_4^0$  and  $\text{Ca}_2\text{Gluc}_2\text{OH}_4^{2-}$  complex is not  
208 important at low calcium concentrations (i.e. the conditions used in this study for the potentiometric  
209 titration) but in the presence of portlandite. Thus their constants were refined using the solubility  
210 data of portlandite.

211 The  $\text{CaSorb}^{2+}$ ,  $\text{CaMan}^{2+}$ , and  $\text{CaGal}^{2+}$  complexes reported in the literature were not found to be in  
212 significant quantities in any of our experiments, as they were obtained in near neutral pH  
213 conditions. Furthermore, the reported values of the complex formation constants are rather  
214 scattered, maybe due to the different methods employed to determine them. We thus introduced in  
215 addition  $\text{CaHexitolOH}^+$  complexes, which were found to give a very satisfactory description of our  
216 experimental data. As it will be described in the next section, the complexation of calcium by the  
217 hexitols is much weaker than by gluconate. The so-obtained complexation constants are compiled  
218 together with the literature values in Table 1 and 2.

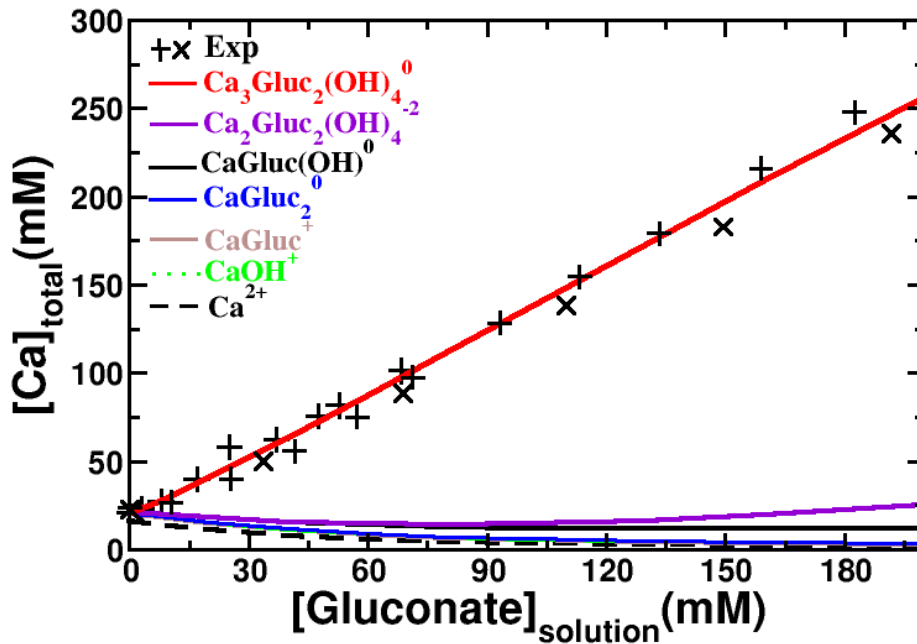
219

## 220 3. Results and discussion

### 221 3.1 Gluconate

#### 222 3.1.1 Solubility experiment with portlandite

223



224 Figure 4: Evolution of total calcium concentrations in equilibrium with portlandite (initial pH 12.6,  
225 final pH 12.8) as a function of the gluconate concentration. The crosses represent the total  
226 concentrations determined experimentally, while the solid lines represent the cumulative calcium  
227 complexes concentrations calculated using the data compiled in Table 1.  
228

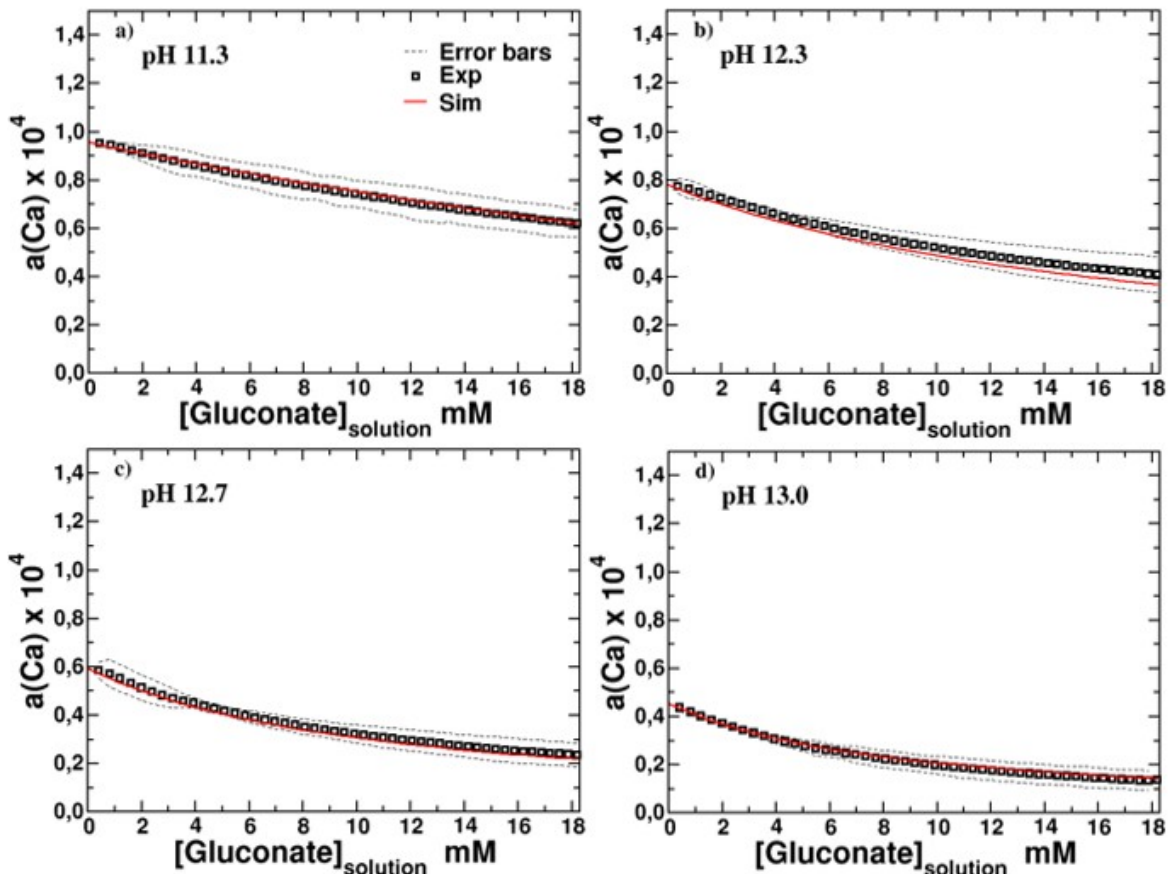
229 The calcium concentrations in equilibrium with portlandite rise rapidly (Figure 4), when the  
230 gluconate concentration is increased. In the absence of gluconate, a calcium concentration of 21  
231 mM was observed, which corresponds well with the expected solubility of portlandite of 21 mM at  
232 23°C. The presence of gluconate increased the total measured calcium concentrations up to 101 mM  
233 Ca at a gluconate concentration of 68 mM, due to the formation of different Ca-gluconate  
234 complexes as shown in Figure 4. This strong increase of portlandite solubility in the presence of  
235 gluconate agrees well with observations reported by Nalet and Nonat (19). The measured increase  
236 of the total calcium concentrations ( $[Ca]_{total} = [Ca^{2+}] + [CaOH^+] + [Ca\text{-organic}]$ ) is mainly due to the  
237 formation of  $Ca_3GluC_2(OH)_4^0$ ,  $CaGluC(OH)_4^0$  and  $Ca_2GluC_2(OH)_4^{2-}$  in presence of gluconate, while our  
238 calculations indicate that the concentrations of  $CaGluC^+$ , and  $CaGluC_2^0$  are negligible. The over-  
239 proportional increase of calcium (80 mM more calcium in solution in the presence of 68 mM

240 gluconate) is consistent with the presence of the heteropolynuclear complex  $\text{Ca}_3\text{Gluc}_2(\text{OH})_4^0$ , which  
 241 contains more calcium than gluconate. At gluconate concentrations of above 20 mM the  
 242  $\text{Ca}_3\text{Gluc}_2(\text{OH})_4^0$  complex dominates Ca-speciation in the presence of portlandite as shown in Figure  
 243 4.

244

### 245 3.1.2 Ca-gluconate titration

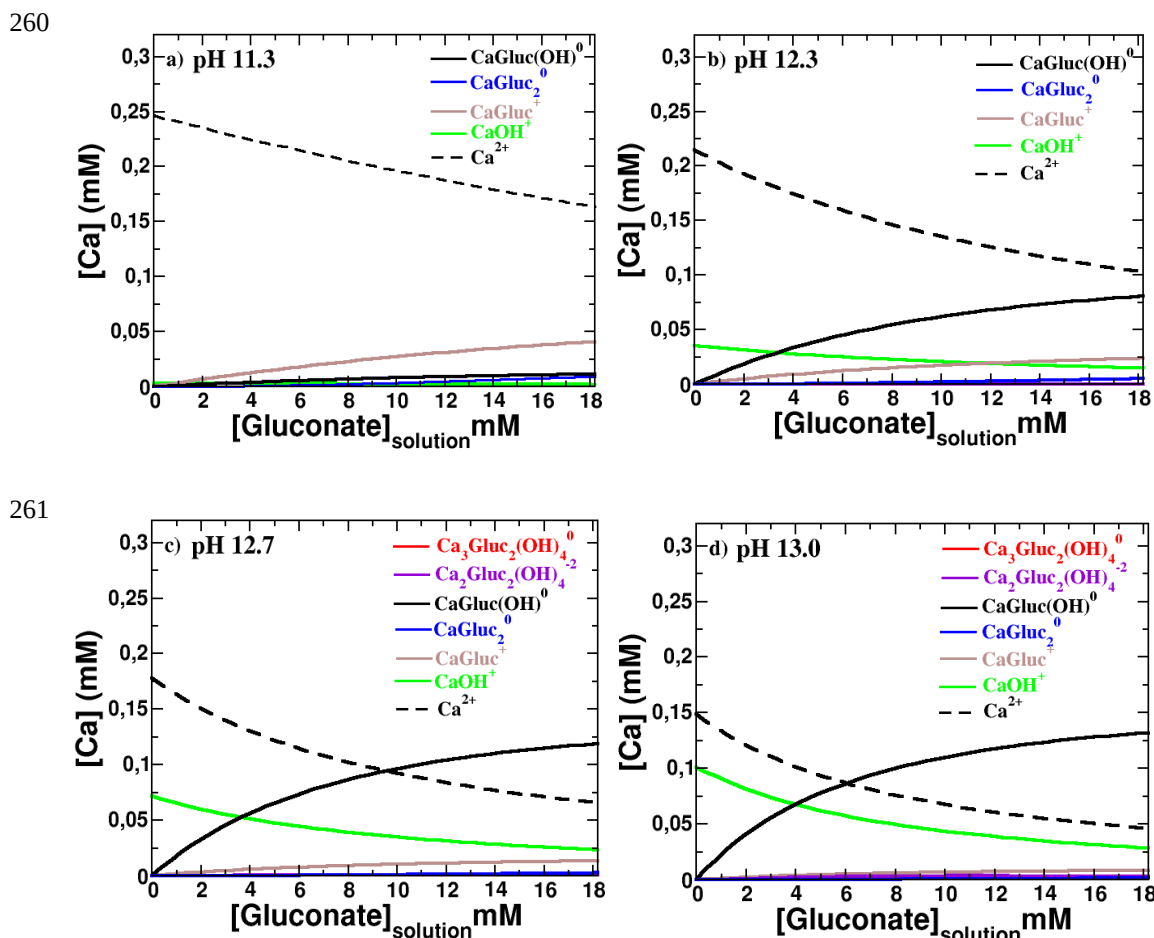
246



247 Figure 5:  $\text{Ca}^{2+}$  activities,  $a_{\text{Ca}}$ , in a solution containing 0.25 mM  $\text{Ca}(\text{NO}_3)_2$  and increasing amounts of  
 248 200 mM K-gluconate solution at pH a) 11.3, b) 12.3, c) 12.7 and d) 13.0. The dots indicate the  
 249 mean of three repetitions of the measurements and the dotted lines the observed standard deviations.  
 250 The solid red lines show the modeled  $a_{\text{Ca}}$  based on the data compiled in Table 1.  
 251

252 The measured changes of the  $\text{Ca}^{2+}$  activity at various alkaline pH values upon the addition of  
 253 potassium gluconate to a solution containing 0.25 mM calcium nitrate is shown in Figure 5. The  
 254 drop of the measured  $\text{Ca}^{2+}$  activity can be attributed i) to a minor extent to the dilution of the  
 255 solution by the addition of the titrant solution (for the effect of adding solution without organics see  
 256 SI) and ii) to the complexation of  $\text{Ca}^{2+}$  with the added gluconate. As it can be seen in Fig. 5 a very

256 good fit of the experimental data with our speciation model is obtained at all pH values. It can also  
 257 be observed that the decrease in calcium activity is limited at pH 11.3 but more distinct at higher pH  
 258 values, which points towards the importance of calcium-gluconate-hydroxide complexes, as further  
 259 confirmed below.



262 Figure 6: Calculated calcium concentrations (in mM) in a solution of 0.25 mM  $\text{Ca}(\text{NO}_3)_2$  during the  
 263 titration with 200 mM K-gluconate at pH a) 11.3, b) 12.3, c) 12.7 and d) 13.0. The calculations are  
 264 based on the thermodynamic data compiled in Table 1.

265

266 In Figure 6 the simulated change in the calcium speciation in the same conditions as in Figure 5 is  
 267 given. In contrast in the solubility experiments, where high calcium concentrations (21 up to 100  
 268 mM Ca, see Figure 4) are present and the calcium complexation is dominated by the  
 269 heteropolynuclear  $\text{Ca}_3\text{Gluc}_2\text{OH}_4^0$  complex,  $\text{CaGluc}^+$  and  $\text{CaGlucOH}^0$  are the dominant complexes at  
 270 the low Ca concentrations used in the titration experiments. For the titration at pH 11.3 mainly the  
 271 formation of some  $\text{CaGluc}^+$  is predicted, while at pH 13.0 the formation of  $\text{CaGlucOH}^0$  is  
 272 principally found, illustrating the strong influence of pH on the calcium speciation. In addition, it

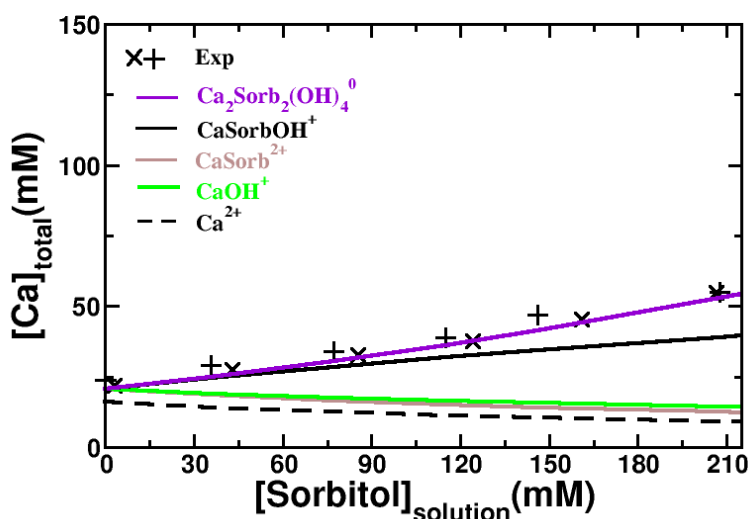
271 can be noted that calcium shows a strong preference for the heterogeneous complex  $\text{CaGlucOH}^0$ ,  
 272 whose concentration is 5 times higher in the presence of 18.8 mM gluconate than that of  $\text{CaOH}^+$  at  
 273 pH 13 ( $\sim 100\text{mM OH}^-$ ). Very low concentrations of the heteropolynuclear complexes,  
 274  $\text{Ca}_2\text{Gluc}_2(\text{OH})_4^{2-}$  and  $\text{Ca}_3\text{Gluc}_2(\text{OH})_4^0$ , were observed due to the relative low Ca (0.25 mM) and  
 275 gluconate (18.8 mM) concentrations, at high pH (12.7 and 13.0).

276

### 277 3.2 Sorbitol

#### 278 3.2.1 Solubility experiments with portlandite

279



280 Figure 7: Evolution of the total calcium concentration in equilibrium with portlandite as a function  
 281 of the sorbitol concentration. The crosses represent the total calcium concentrations determined  
 282 experimentally, while the lines represent the calcium concentrations calculated using the data  
 283 compiled in Table 2. The cumulative calcium concentrations due to  $\text{Ca}^{2+}$  (black, dashed line),  
 284  $\text{CaOH}^+$  (green, solid line),  $\text{CaSorb}^{2+}$  (grey, solid line),  $\text{CaSorbOH}^+$  (black, solid line) and  
 285  $\text{Ca}_2\text{Sorb}_2(\text{OH})_4^0$  (purple, solid line) are also plotted.

286

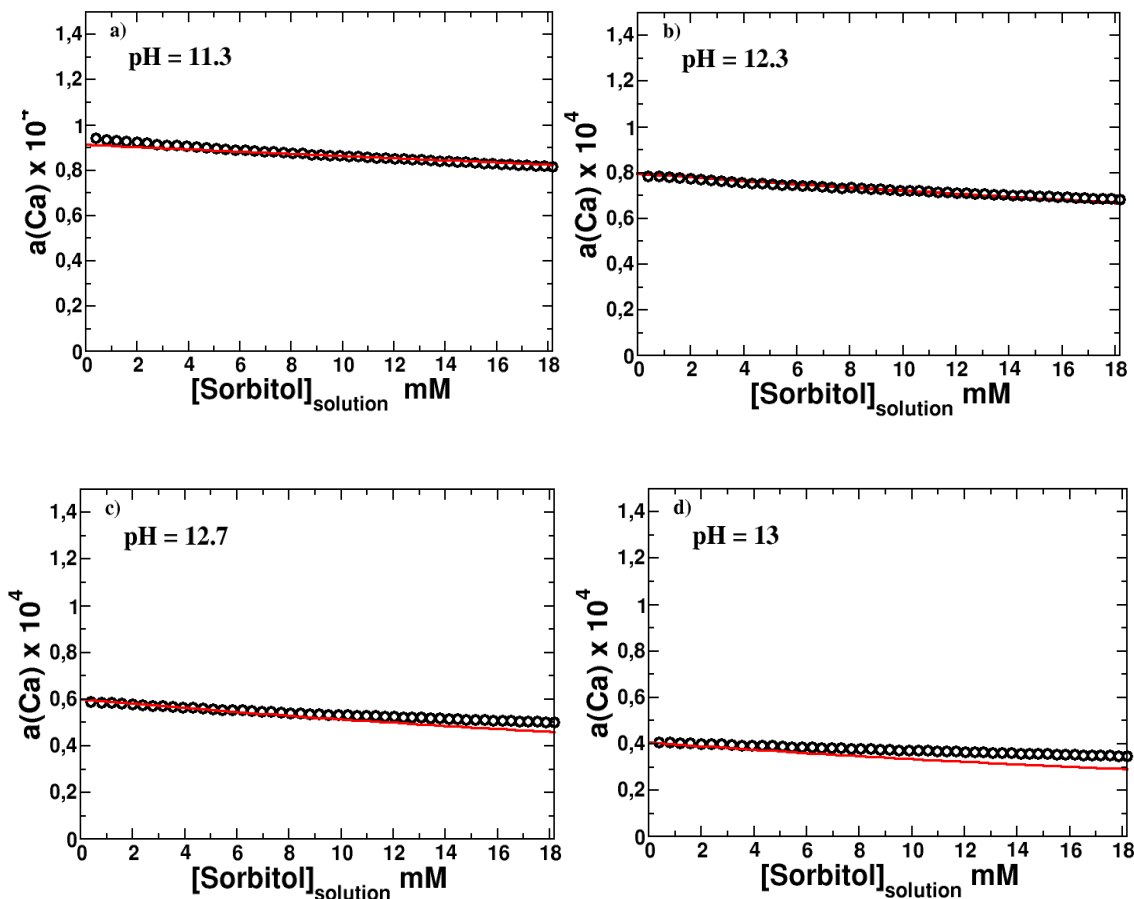
287 The equilibrium calcium concentration as obtained in the solubility experiments of portlandite in  
 288 the presence of sorbitol is given in Figure 7. The equilibrium calcium concentration is observed to  
 289 increase moderately with that of sorbitol, from 21 mM to 55 mM when sorbitol is increased up to  
 290 211 mM. The increase is much weaker than the one due to gluconate (Figure 4), indicating a weaker  
 291 complex formation between  $\text{Ca}^{2+}$  and sorbitol. The calculations show that the observed increase can  
 292 be mainly explained by the formation of a  $\text{CaSorbOH}^+$  complex, while the concentration of  
 293  $\text{CaSorb}^{2+}$  is found to be negligible. No clear indication for the formation of polynuclear complexes

294 is found, although the underestimation of the total calcium concentration at very high sorbitol  
 295 concentrations could point towards the formation of such complex. At sorbitol concentrations of  
 296 100 mM and above, the  $\text{CaSorbOH}^+$  complex dominates Ca-speciation (Figure 7).

297

### 298 3.2.2 Ca-sorbitol titration

299



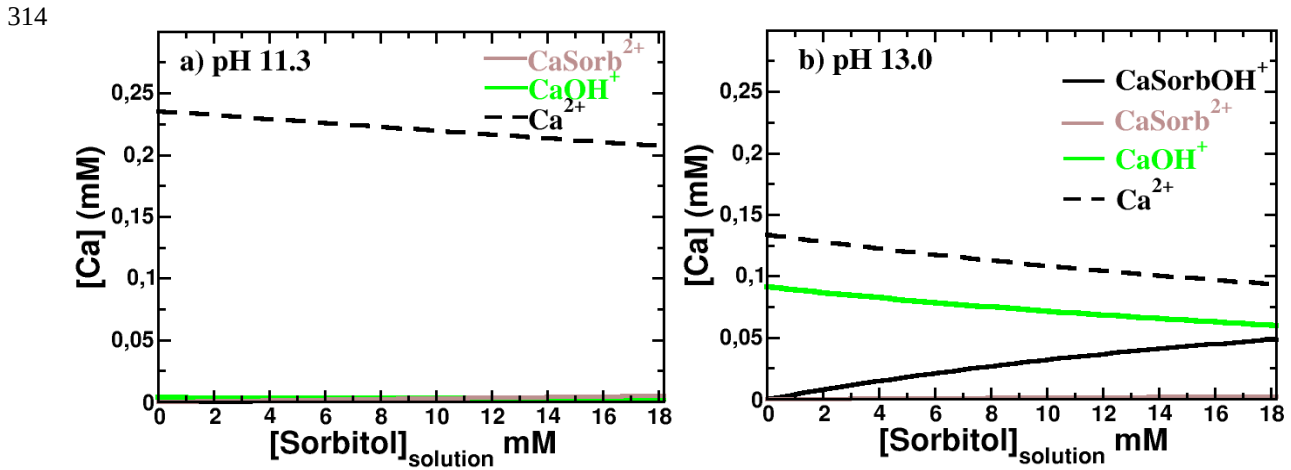
300

301 Figure 8:  $\text{Ca}^{2+}$  activities,  $a_{\text{Ca}^{2+}}$ , in a solution containing 0.25 mM  $\text{Ca}(\text{NO}_3)_2$  and increasing amounts  
 302 of 0.2 M sorbitol solution at pH a) 11.3, b) 12.3, c) 12.7 and d) 13.0. The solid red lines show the  
 303 modeled  $a_{\text{Ca}^{2+}}$  based on the data compiled in Table 2.

304

305 The change in the activity of  $\text{Ca}^{2+}$  at different pH values upon the addition of sorbitol as measured  
 306 by potentiometric titration of a diluted calcium nitrate solution (0.25 mM) is shown in Figure 8. In  
 307 agreement with the solubility experiments (Fig.7), the drop of the  $\text{Ca}^{2+}$  activity is weaker than the  
 308 one observed with gluconate and more distinct at high pH values as explained by the formation of  
 309  $\text{CaSorbOH}^+$  complex. This is illustrated in Figure 9, which provides the detailed calculated  
 310 speciation of calcium. As expected,  $\text{CaSorbOH}^+$  is prevalent at pH 13 and hardly visible at pH 11.3.

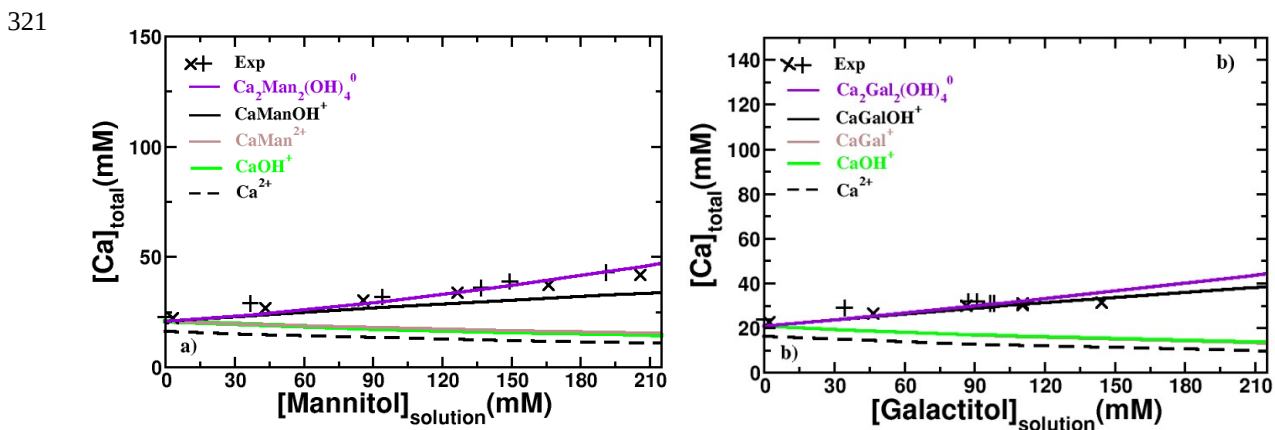
310 In line with the solubility experiments, the  $\text{CaSorb}^{2+}$  complex is negligible in these alkaline  
 311 conditions. The overall good agreement obtained between modeled and experimentally observed  
 312 decrease of the  $\text{Ca}^{2+}$  activities clearly shows that no or only very little polynuclear Ca-sorbitol  
 313 complexes are present.



315 Figure 9: Calcium concentrations (in mM) in a solution of 0.25 mM  $\text{Ca}(\text{NO}_3)_2$  during the titration  
 316 with sorbitol at a) pH 11.3 and b) pH 13.0 calculated based on the thermodynamic data compiled in  
 317 Table 2.

318  
 319 **3.3 Mannitol and galactitol**

320 *3.3.1 Solubility experiments with portlandite*



322 Figure 10: Evolution of calcium concentrations in equilibrium with portlandite at a pH value of 12.6  
 323 as a function of a) mannitol and b) galactitol concentration. The crosses represent the total calcium  
 324 concentrations determined experimentally, while the lines represent the calcium concentrations  
 325 calculated using the thermodynamic data compiled in Table 2. The cumulative calcium  
 326 concentrations of  $\text{Ca}^{2+}$  (black, dashed line),  $\text{CaOH}^+$  (green, solid line),  $\text{CaMan}^{2+}$  or  $\text{CaGal}^{2+}$  (grey,  
 327 solid line),  $\text{Ca}_2\text{Man}_2(\text{OH})_4^0$  or  $\text{Ca}_2\text{Gal}_2(\text{OH})_4^0$  (purple, solid line) and  $\text{CaManOH}^+$  or  $\text{CaGalOH}^+$   
 328 (black, solid line) are also plotted.

329

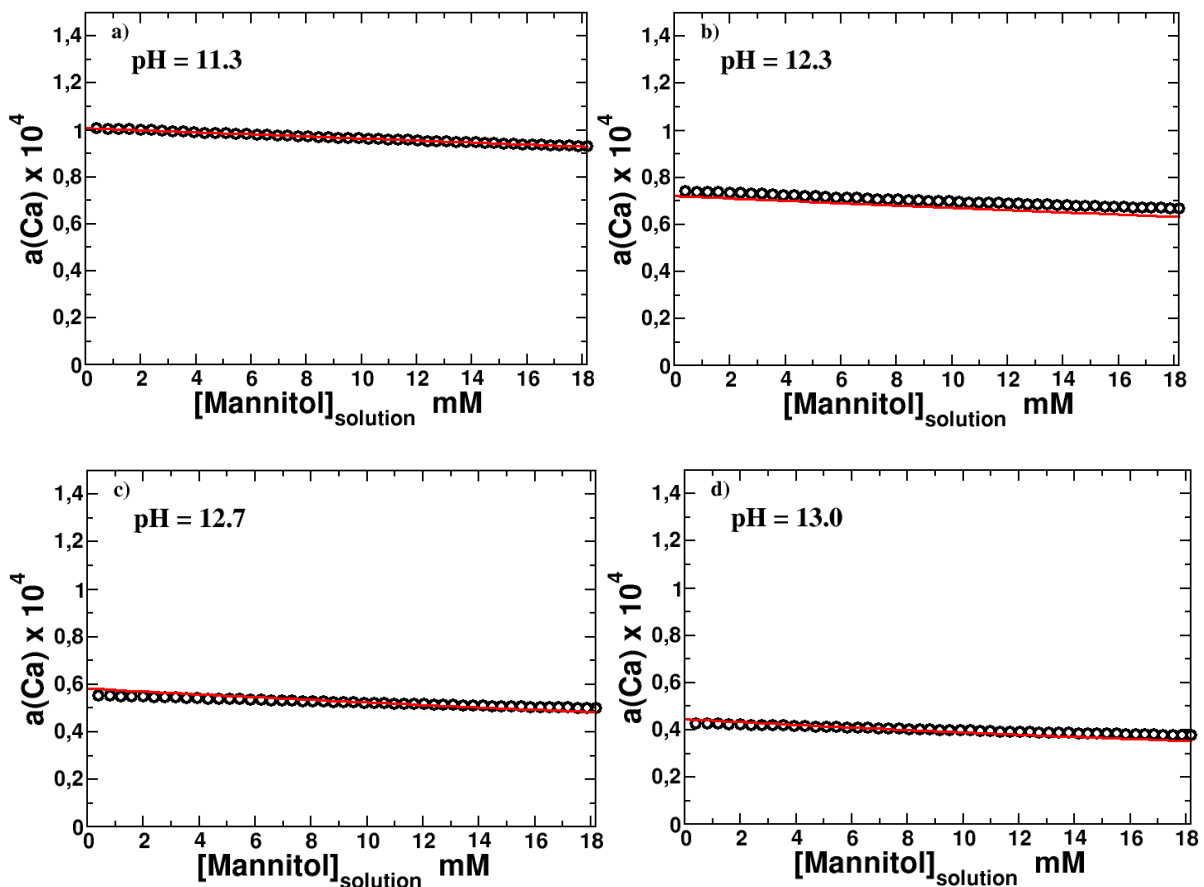


330 The increase in the equilibrium calcium concentration in the solubility experiments of portlandite in  
 331 the presence of mannitol and galactitol, given in Figure 10, is comparable to that observed with  
 332 sorbitol, although somewhat weaker compared with Figure 7. As for sorbitol, the observed increase  
 333 of the Ca concentration can be principally explained by the formation of  $\text{CaManOH}^+$  and  
 334  $\text{CaGalOH}^+$  complexes, while the concentrations of  $\text{CaMan}^{2+}$  and  $\text{CaGal}^{2+}$  are negligible. Only at  
 335 mannitol and galactitol concentrations well above 100 mM,  $\text{CaManOH}^+$  and  $\text{CaGalOH}^+$  complexes  
 336 dominate the speciation of calcium (Figure 10).

337

### 338 3.3.2 Ca-mannitol and Ca-galactitol titration

339



340

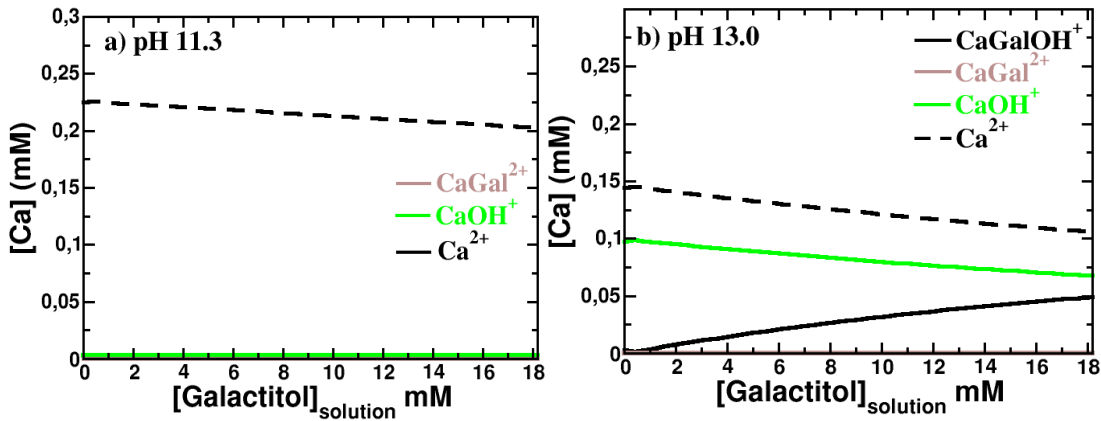
341 Figure 11:  $\text{Ca}^{2+}$  activities,  $a_{\text{Ca}^{2+}}$ , in a solution containing 0.25 mM  $\text{Ca}(\text{NO}_3)_2$  and increasing  
 342 amounts of 0.2 M mannitol solution at pH a) 11.3, b) 12.3, c) 12.7 and d) 13.0. The experimental  
 343 points are shown by the empty circles. The solid red lines give the modeled  $a_{\text{Ca}^{2+}}$ , based on the data  
 344 compiled in Table 2, for comparison.

345

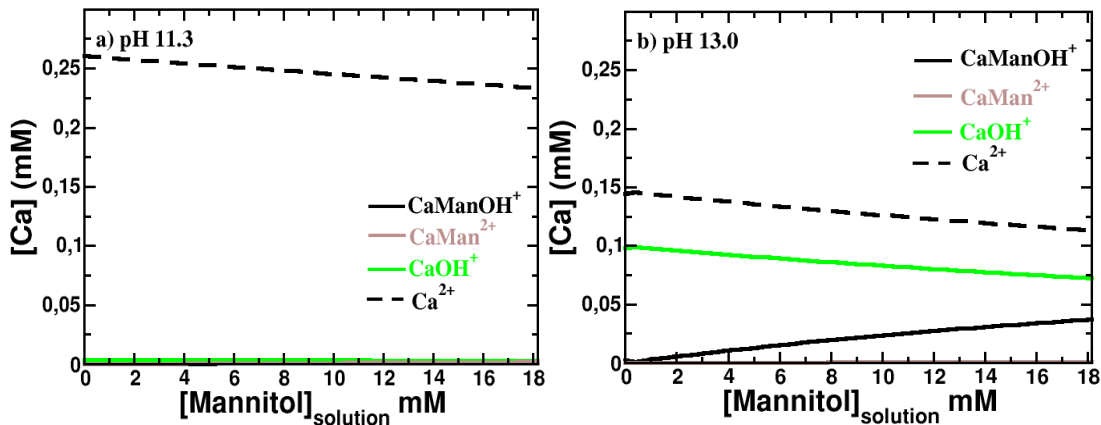
346 The change in the simulated and measured activity of  $\text{Ca}^{2+}$  and pH upon the addition of 0 to 18 mM  
 347 mannitol to a 0.25 mM calcium nitrate at pH 11.3, 12.3, 12.7 and 13.0 are shown in Figure 11. The

348 data for galactitol are similar and provided in the supplementary information. In agreement with the  
 349 solubility experiments of portlandite (Figure 10), the decrease in the measured  $a_{Ca^{2+}}$  is less  
 350 pronounced than in the case of sorbitol and is mainly explained by the formation  $CaManOH^+$  and  
 351  $CaGalOH^+$  at higher pH values. The strong preference of calcium for the heterogeneous complex  
 352 with hydroxide ( $CaManOH^+$  and  $CaGalOH^+$ ) is further illustrated in Figure 12.

353



354



355 Figure 12: Simulated speciation of calcium in a solution of 0.25 mM  $Ca(NO_3)_2$  during the titration  
 356 with above a) galactitol at pH 11.3 and b) galactitol at pH 13.0, and below, a) mannitol at pH 11.3  
 357 and b) mannitol at pH 13.0. The calculations are based on the thermodynamic data compiled in  
 358 Table 2.

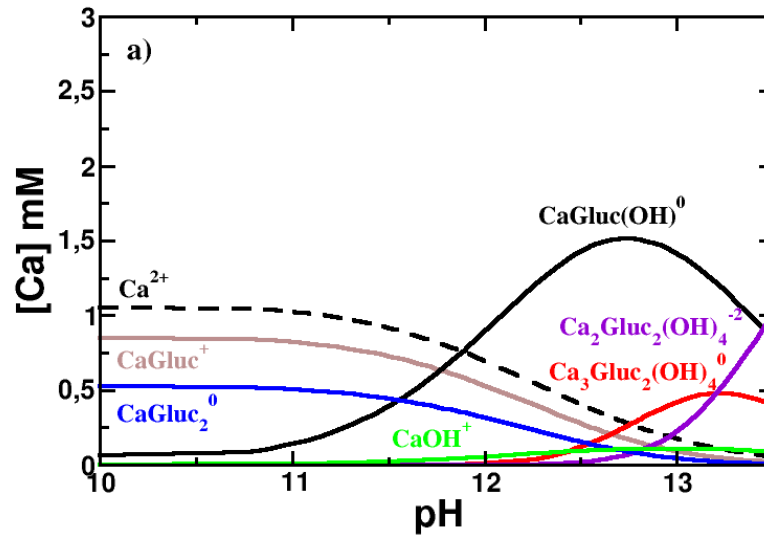
359

### 360 3.4 Effect of complexation on calcium speciation

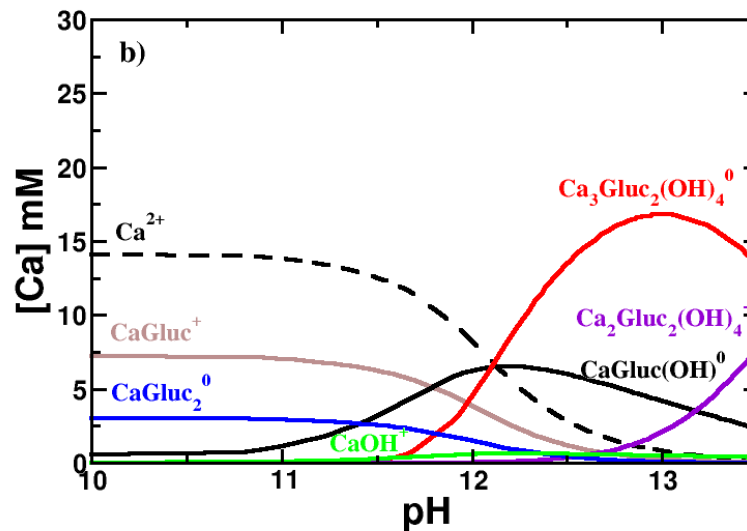
361 Calcium has been observed to form a number of different complexes with gluconate and hydroxide.  
 362 Under conditions relevant for the early-age pore solution of cements (10-40 mM Ca, pH 12.5 -13.5)  
 363 mainly the  $CaGlucOH^0$ ,  $Ca_3Gluc_2(OH)_4^0$  and  $Ca_2Gluc_2(OH)_4^{-2}$  complexes are of importance as  
 364 illustrated in Figure 13b. The importance of  $CaGlucOH^0$ ,  $Ca_3Gluc_2(OH)_4^0$  and  $Ca_2Gluc_2(OH)_4^{-2}$   
 365 complexes at pH values above 12.5 result in much lower concentrations of free  $Ca^{2+}$  than in the

365 absence of gluconate. The effect can be expected to be even stronger at later hydration times, where  
 366 calcium concentrations drop to a few mM, while the concentrations of small organic molecules in  
 367 the pore solutions tend to remain high. This leads to a stabilization of  $\text{CaGlucOH}^0$  as shown in  
 368 Figure 13a and lower  $\text{Ca}^{2+}$  concentrations.

369



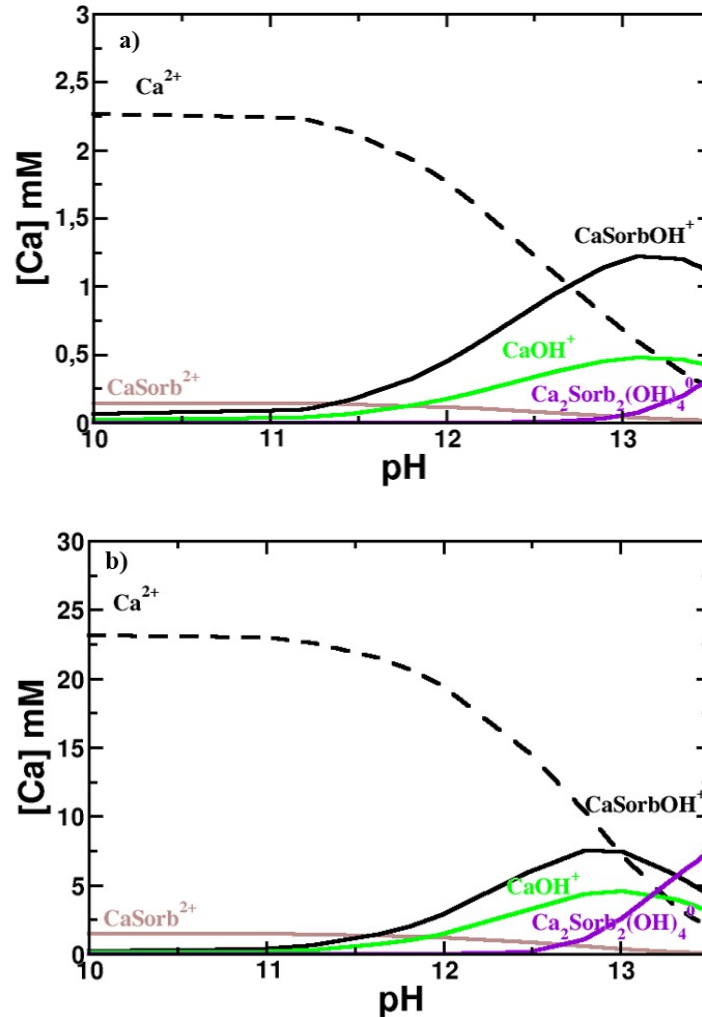
370



371 Figure 13: Calcium distribution (expressed as mM Ca) in a solution containing a) 2.5 mM of Ca , b)  
 372 25 mM of Ca and 50 mM of gluconate in the pH range 10 to 13.5.  
 373

374 The strong complexation of calcium can be expected to retard portlandite and C-S-H precipitation  
 375 during cement hydration. Gluconate sorbs also strongly on calcium at the surface of  $\text{C}_3\text{S}$ , portlandite  
 376 (see Supplementary Information) and C-S-H (18) (19), which will also strongly influence their  
 377 dissolution and formation rate.

378 Calcium forms only relatively weak complexes with the three hexitols investigated, in the order  
 379 sorbitol > mannitol > galactitol. Thermodynamic modelling indicates a non negligible Ca-  
 380 complexation in conditions relevant for the pore solution of cements (10-40 mM Ca, pH 12.5 -13.5)  
 381 as illustrated for sorbitol in Figure 14.  
 382



383

384 Figure 14: Calcium distribution (expressed as mM Ca) in a solution containing a) 2.5 mM of Ca, b)  
 385 25 mM of Ca and 50 mM of sorbitol in the pH range 10 to 13.5.  
 386

387 The observed tendency of calcium to form complexes with organics follows the order gluconate >>  
 388 sorbitol > mannitol > galactitol, which corresponds well with the tendency to sorb on portlandite  
 389 (see Supplementary informations) and C-S-H (18) (19): gluconate >> sorbitol > mannitol, but only  
 390 partially with their tendency to retard the C<sub>3</sub>S hydration reported in Nalet and Nonat (15): gluconate  
 391 >> sorbitol > galactitol > mannitol. The reason for the different sequence of galactitol and mannitol

392 on C<sub>3</sub>S hydration is presently not clear. The charged gluconate, which complexed strongly with  
393 calcium in solution had also the biggest retarding effect on C<sub>3</sub>S hydration.

394

#### 395 **4. Conclusions**

396 The complexation of Ca<sup>2+</sup> with gluconate, D-sorbitol, D-mannitol and D-galactitol has been studied  
397 via portlandite solubility measurement and titration experiments at low ionic strength (0.1 M  
398 KNO<sub>3</sub>).

399 For gluconate, the multinuclear complexes already described in the literature allowed us to describe  
400 the experimental data, after some further refinement of the complexation constants. At a pH of 12.5  
401 and in the presence of portlandite the heteropolynuclear complex Ca<sub>3</sub>Gluc<sub>2</sub>(OH)<sub>4</sub><sup>0</sup> dominates the  
402 Ca-speciation, while at lower calcium concentrations CaGluc<sup>+</sup> (below pH 12) and CaGlucOH<sup>0</sup>  
403 (above pH 12) are the main complexes formed. This relative strong complex formation between  
404 calcium and gluconate lowers concentrations of free Ca<sup>2+</sup>, which could contribute to a retardation of  
405 portlandite and C-S-H precipitation during cement hydration. The strong tendency of gluconate to  
406 form complexes with Ca reported here is consistent with the significant sorption of gluconate on Ca  
407 on the surface of C-S-H and portlandite reported (19) .

408 Sorbitol makes weaker complexes with calcium as observed both from portlandite solubility  
409 measurements and titration results. Under all conditions studied, the predominant sorbitol complex  
410 is the ternary CaSorbOH<sup>+</sup> complex, while the CaSorb<sup>2+</sup> complex formed in negligible amounts  
411 only. In all cases studied, CaSorbOH<sup>+</sup> complex had limited effect on calcium speciation below a pH  
412 of 12, but can dominate the calcium speciation at pH 12.5 and above, at higher sorbitol  
413 concentrations.

414 Similar observations have been made for D-mannitol and D-galactitol, which show an even weaker  
415 tendency than sorbitol to form calcium complexes. Also, for D-mannitol and D-galactitol only the  
416 ternary CaManOH<sup>+</sup> and CaGalOH<sup>+</sup> complexes are relevant, and they are expected to form mainly  
417 above pH 12.5 and at high mannitol and galactitol concentrations.

418 The observed tendency of calcium to form complexes follows the order gluconate >> sorbitol >  
419 mannitol > galactitol, which corresponds well with the tendency to sorb on portlandite and C-S-H:  
420 gluconate >> sorbitol > mannitol (19) but only partially with their tendency to retard the C<sub>3</sub>S  
421 hydration reported in (15): gluconate >> sorbitol > galactitol > mannitol.

422

## 423 **Acknowledgements**

424 The financial support from Nanocem (core project 15) is thankfully acknowledged. We also would  
425 like to thank the representatives of the industrial partners: L. Pegado, J.H. Cheung, V. Kocaba, P.  
426 Juilland, and M. Mosquet for many helpful discussions and their interest in this project. We  
427 sincerely thank L. Brunetti, S. El Housseini and D. Nguyen for their help in the laboratory work.  
428 The use of the analytical platform of ISTerre, with the help of D. Tisserand, S. Bureau and S.  
429 Campillo, is acknowledged.

430

## 431 **References**

- 432 1. Mann.S. *Biom mineralization: Principles and Concepts in Bioorganic Materials Chemistry*. Oxford  
433 University Press, Oxford, New York. 2001.
- 434 2. Jolicoeur.C., Simard.M.A. Chemical admixture-cement interactions: phenomenology and  
435 physico-chemical concepts. *Cement and Concrete Composites*, 20(2–3), 87-101. 1998.
- 436 3. Young.J.F. A review of the mechanisms of set-retardation in portland cement pastes containing  
437 organic admixtures. *Cement and Concrete Research*, 2(4), 415-433. 1972.
- 438 4. Lorprayoon.V., Rossington.D.R. Early hydration of cement constituents with organic admixtures.  
439 *Cement and Concrete Research*, 11(2), 267-277. 1981.
- 440 5. Uchikawa.H., Hanehara.S., Shirasaka.T., Sawaki.D. Effect of admixture on hydration of cement,  
441 adsorptive behavior of admixture and fluidity and setting of fresh cement paste. *Cement and*  
442 *Concrete Research*, 22(6), 115-1129. 1992.
- 443 6. Jansen.D., Neubauer.J., Goetz-Neunhoeffler.F., Haerzschel.R., Hergeth.W.D. Change in reaction  
444 kinetics of a portland cement caused by a superplasticizer — Calculation of heat flow curves from  
445 XRD data. *Cement and Concrete Research*, 42(2), 327-332. 2012.
- 446 7. Cheung.J., Jeknavorian.A., Robert.L., Silva.D. Impact of admixtures on the hydration kinetics of  
447 Portland cement. *Cement and Concrete Research*, 41(12), 1289-1309. 2011.
- 448 8. Diamond.S. Interactions between cement minerals and hydroxycarboxylic-acid retarders: I,  
449 apparent adsorption of salicylic acid on cement and hydrated cement compounds. *Journal of the*  
450 *American Ceramic Society*, 54(6), 273-276. 1971.
- 451 9. Nelson.E.B. Cements additives and mechanisms of action. *Well Cementing*, 28, 3-1-3-37. 1990.
- 452 10. Milestone.N.B. Hydration of tricalcium silicate in the presence of lignosulfonates, glucose, and  
453 sodium gluconate. *Journal of the American Ceramic Society*, 62(8), 321-326. 1979.
- 454 11. Singh.N.B., Singh.S.P., Sarvehi.R. Effect of phenols on the hydration of Portland cement.  
455 *Advances in Cement Research*. 2(6), 43-48. 1989.

- 456 12. Zhang.L., Catalan.L.J.J., Balec.R.J., Larsen.A.C., Esmaili.H.H. and Kinrade.S.D. Effect of  
457 saccharide set retarders on the hydration of ordinary portland cement and pure tricalcium silicate.  
458 *Journal of the American Ceramic Society*, 93 (1) 279–287. 2010.
- 459 13. Thomas.J.J., Jennings.H.M., Chen.J.J. Influence of nucleation seeding on the hydration  
460 mechanisms of tricalcium silicate and cement. *Journal of Physical Chemistry*, 113(11), 4327-4334.  
461 2009.
- 462 14. Pourchez.J., Grosseau.P., Ruot.B. Changes in C<sub>3</sub>S hydration in the presence of cellulose ethers.  
463 *Cement and Concrete Research*, 40(2), 179–188. 2010.
- 464 15. Nalet.C., Nonat.A. Effects of hexitols on the hydration of tricalcium silicate. *Cement and*  
465 *Concrete Research*, 91, 87-96. 2017.
- 466 16. Nalet.C., Nonat.A. Effects of functionality and stereochemistry of small organic molecules on  
467 the hydration of tricalcium silicate. *Cement and Concrete Research*, 87, 97-104. 2016.
- 468 17. Juilland.P., Gallucci.E. Hindered calcium hydroxide nucleation and growth as mechanism  
469 responsible for tricalcium silicate retardation in presence of sucrose. 329, 143-154. 2018.
- 470 18. Hansen, W. Actions of calcium sulfate and admixtures in portland cement pastes in "symposium  
471 on effect of water-reducing admixtures and set-retarding admixtures on properties of concrete".  
472 *American Society for Testing Materials* 3-37. 1960.
- 473 19. Nalet.C., Nonat.A. Ionic complexation and adsorption of small organic molecules on calcium  
474 silicate hydrate: relation with their retarding effect on the hydration of C<sub>3</sub>S. *Cement and Concrete*  
475 *Research*, 89, 97–108. 2016.
- 476 20. Singh.N.B. Influence of calcium gluconate with calcium chloride or glucose on the hydration of  
477 cements. *Cement and Concrete Research*, 5, 545-550. 1975.
- 478 21. Singh.N.B. Effect of gluconate on the hydration of cement. *Cement and Concrete Research*, 6,  
479 455-460. 1976.
- 480 22. Ma.S., Li.W., Zhang.S., Ge.D., Yu.J., Shen.X. Influence of sodium gluconate on the  
481 performance and hydration of portland cement. *Construction and Building Materials*, 91, 138-144.  
482 2015.
- 483 23. Pallagi.A., Sebők.P., Forgó.P., Jakusch.T., Pálkó.I., Sipos.P. Multinuclear NMR and  
484 molecular modelling investigations on the structure and equilibria of complexes that form in  
485 aqueous solutions of Ca<sup>2+</sup> and gluconate. *Carbohydrate Research*, 345(13), 1856-1864. 2010.
- 486 24. Pallagi.A., Bajnóczi.É.G., Canton.S.E., Bolin.T., Peintler.G., Kutus.B., Sipos.P. Multinuclear  
487 complex formation between Ca(II) and gluconate ions in hyperalkaline solutions. *Environmental*  
488 *Science & Technology*, 48(12), 6604-6611. 2014.
- 489 25. Kutus.B., Ozsvár.D., Varga.N., Pálkó.I., Sipos.P. ML and ML2 complexes forming between  
490 Ca(II) and D-glucose derivatives in aqueous solutions. *Dalton Transactions*, 46, 1065-1074. 2017.
- 491 26. Kutus.B., Gaona.X., Pallagi.A., Pálkó.I., Altmaier.M., Sipos.P., Recent advances in the  
492 aqueous chemistry of the calcium(II)-gluconate system - Equilibria, structure and composition of  
493 the complexes forming in neutral and in alkaline solutions. *Coordination Chemistry Reviews*, 417,  
494 213337. 2020.
- 495 27. Masone.M., Vicedomini.M. Gluconate and lactate as ligand of calcium ions. 71(9-10), 517-523.  
496 1981.
- 497 28. Sawyer, D.T. Metal organic complexes. *Chemical Reviews*, 64(6), 633-643. 1964.
- 498 29. Haas.J.W. Complexation of calcium and copper with carbohydrates. *Marine Chemistry*, 19(4),  
499 299-304. 1986.
- 500 30. Kieboom.A.P.C, Buurmans.H.M.A, Van Leeuwen.L.K., Van Benschop.H.J. Stability constants  
501 of (hydroxy)carboxylate and alditol-calcium(II) complexes in aqueous medium as determined by a  
502 solubility method. *Journal of the Royal Netherlands Chemical Society*, 98(6), 393-394. 1979.
- 503 31. Barthel.J., Jaenicke.R. Conway: Ionic Hydration in Chemistry and Biophysics: Studies in  
504 Physical and Theoretical Chemistry. Elsevier Scientific Publishing Company, 86(3), 264-264,  
505 Amsterdam and New York. 1982.
- 506 32. Parkhurst.D.L. PHREEQE: a computer program for geochemical calculations. U.S. Geological  
507 Survey, Water Resources Division, 80-96. 1981.

- 508 33. Ball.J.W., Nordstrom.D.K. User's Manual for WATEQ4F, with Revised Thermodynamic Data  
509 Base and Test Cases for Calculating Speciation of Major, Trace, and Redox Elements in Natural  
510 Waters. U.S. Geological Survey, 91-183, Washington DC. 1991.
- 511 34. Merkel.B., Planer-Friederich.B., Nordstrom.D. Groundwater Geochemistry. A Practical Guide  
512 to Modeling of Natural and Contaminated Aquatic Systems. Springer. 2005.
- 513 35. Zhang.Z., Gibson.P., Clark.S.B., Tian.G., Zanonato.P.L., Rao.L. Lactonization and protonation  
514 of gluconic acid: a thermodynamic and kinetic study by potentiometry, NMR and ESI-MS. Journal  
515 of Solution Chemistry, 36(10), 1187-1200. 2007.
- 516 36. Bretti.C., Cigala.R.M., De Stefano.C., Lando.G., Sammartano.S. Acid–base and thermodynamic  
517 properties of D-gluconic acid and its interaction with Sn<sup>2+</sup> and Zn<sup>2+</sup>. Journal of Chemical and  
518 Engineering Data, 61(6), 2040–2051. 2016.
- 519 37. Thoenen.T., Hummel.W., Berner.U., Curti.E., The PSI/Nagra Chemical Thermodynamic Data  
520 Base 12/07, PSI report 14-04, Villigen PSI, Switzerland. 2014  
521